Atomistic simulations of the incipient ferroelectric $KTaO_3$

A. R. Akbarzadeh,[1] L. Bellaiche,[1] Kevin Leung,[2] Jorge Íñiguez,[3,4,5] and David Vanderbilt[3]
[1]*Physics Department, University of Arkansas, Fayetteville, Arkansas 72701, USA*
[2]*Sandia National Laboratories, Mail Stop 1421, Albuquerque, New Mexico 87185, USA*
[3]*Department of Physics and Astronomy, Rutgers University, Piscataway, New Jersey 08854-8019, USA*
[4]*NIST Center for Neutron Research, National Institute of Standards and Technology, Gaithersburg, Maryland 20899-8562, USA*
[5]*Department of Materials Science and Engineering, University of Maryland, College Park, Maryland 20742-2115, USA*
(Received 22 December 2003; published 17 August 2004)

A parameterized effective Hamiltonian approach is used to investigate $KTaO_3$. We find that the experimentally observed anomalous dielectric response of this incipient ferroelectric is well reproduced by this approach, once quantum effects are accounted for. Quantum fluctuations suppress the paraelectric-to-ferroelectric phase transition; it is unnecessary to introduce defects to explain the dielectric behavior. The resulting quantum-induced local structure exhibits off-center atomic displacements that display *longitudinal, needle-like correlations* extending a few lattice constants.

DOI: 10.1103/PhysRevB.70.054103 PACS number(s): 77.84.−s, 78.20.Bh, 81.30.Dz

I. INTRODUCTION

Numerous experimental and theoretical studies have been carried out on the perovskite $KTaO_3$ over the last 40 years (see, e.g., Refs. 1–12, and references therein), making this material one of the most-studied "incipient ferroelectrics." The main reason for this interest is that the dielectric constant of $KTaO_3$ increases continuously with decreasing temperature down to ~10 K, but then saturates to a plateau at a large value (≃4000) at lower temperatures while remaining paraelectric and cubic all the way down to 0 K.[2,3] These anomalous low-temperature features are usually thought to be caused by the suppression of a paraelectric-to-ferroelectric phase transition by zero-point quantum fluctuations[2,3] (hence, the name "incipient ferroelectric" or "quantum paraelectric" used to describe $KTaO_3$ and other materials, such as $SrTiO_3$, exhibiting similar unusual dielectric and structural properties). Surprisingly, this generally accepted picture is apparently *not* supported by various first-principles calculations, using the density-functional theory (DFT) either in its local-density approximation (LDA),[13] or generalized-gradient approximation (GGA),[14,15] form since these simulations all predict that $KTaO_3$ should be paraelectric at $T=0$ even when neglecting zero-point motion.[4–6] This raises the possibility that LDA and GGA are not accurate enough to adequately reproduce the qualitative properties of incipient ferroelectrics. An alternate explanation for this discrepancy between first-principles calculations and experiments is that the simulations assume a perfect material while real samples may contain defects such as oxygen vacancies and Fe^{+3} ions,[2,3,7,8] that might lead to the observed anomalous properties of $KTaO_3$. In fact, the interpretation of various experiments,[9,10] still remains controversial as to whether they are attributable to extrinsic effects (i.e., defects induced) or intrinsic off-center atomic displacements. Furthermore, while previous studies invoke the existence of *ferroelectric microregions* inside the *macroscopically-paraelectric* $KTaO_3$ system to explain some of its properties,[9,11] there has never been any *direct* determination of the size and shape of these proposed polar regions, to the best of our knowledge. For instance, the pioneering work of Ref. 9 made several assumptions in their analysis of low-temperature Raman spectra—such as isotropy of these microregions—to extract a characteristic size ≃16 Å for these polar regions.

We use large-scale atomistic simulations to shed light on the aforementioned long-standing problems. We report calculations on $KTaO_3$ using a parameterized effective Hamiltonian approach. Our main findings are that (i) LDA and GGA are indeed not accurate enough to reproduce the observed anomalous properties of $KTaO_3$, even qualitatively; (ii) these properties *can* be understood *without the need of introducing defects*, if quantum fluctuations are present to suppress the paraelectric-to-ferroelectric transition; (iii) the low-temperature local structure of $KTaO_3$ is characterized by off-center atomic displacements that are *longitudinally correlated, in a needle-like (and thus anisotropic) way, with a correlation length spanning a few five-atom unit cells*.

The remainder of this paper is organized as follows. In Sec. II, we give a brief description of the methods we have used. Section III discusses the results on dielectric susceptibility and microscopic properties of $KTaO_3$. Finally, Sec. IV concludes the paper.

II. METHODOLOGY

We use the effective Hamiltonian (H_{eff}) approach developed in Ref. 16 to investigate finite-temperature properties of $KTaO_3$. Within this approach, the total energy E_{tot} is a function of three types of local degrees of freedom: (1) the $\mathbf{u}_i$ (B-site centered) local soft-mode amplitude in each i five-atom cell, describing the local polarization in each cell; (2) the v_i (A-site centered) inhomogeneous strain variables; and (3) the homogeneous strain tensor. E_{tot} contains 18 parameters and 5 different contributions: a local-mode self energy, a long-range dipole-dipole interaction, a short-range interaction between local modes, an elastic energy, and an interaction between the local modes and strains.[16] This effective Hamiltonian approach has been successfully used to model,

understand, and design ferroelectric perovskites (see Refs. 16 and 19–22, and references therein). E_{tot} is used in two different kinds of Monte-Carlo (MC) simulations: classical Monte Carlo (CMC),[23] which does not take into account zero-point phonon vibrations, and path-integral quantum Monte Carlo (PI-QMC),[21,24,25] which includes purely quantum-mechanical zero-point motion. Consequently, comparing the results of these two different Monte-Carlo techniques allows a precise determination of quantum effects on macroscopic and microscopic properties of perovskites. $12\times12\times12$ $KTaO_3$ supercells (corresponding to 8640 atoms) are used in all Monte-Carlo simulations. We typically perform 30 000 MC sweeps to thermalize the system and 70 000 more to compute averages, except at low temperatures in PI-QMC where more statistics is needed. For example, we use 180 000 MC sweeps for thermalization and 240 000 sweeps at 3 K to accurately predict the dielectric response. (Note that we are not aware of any previous work reporting the dielectric response computed using PI-QMC.)

In PI-QMC, each five-atom cell interacts with its images at neighboring imaginary times through a spring-like potential (mimicking the zero-point phonon vibrations), while all the five-atom cells interact with each other at the same imaginary time through the internal potential associated with E_{tot}. The product TP, where T is the simulated temperature and P is the number of imaginary time slices (Trotter number), controls the accuracy of the PI-QMC calculation. In all our simulations we use $TP=600$, which we find leads to sufficiently converged results. Outputs of the PI-QMC simulations thus contain local modes $\boldsymbol{u}_i(t)$, where i indexes the five-atom unit cells of the studied supercell while the imaginary time t ranges between 1 and P. Note that CMC simulations can be thought of as corresponding to $P=1$, so that they do not yield imaginary-time-dependent outputs.

III. RESULTS

Figure 1(a) shows the χ_{33} dielectric susceptibility—where the index 3 refers to the [001] pseudocubic direction—as predicted by the H_{eff} approach, *with all its parameters being derived from LDA calculations on small supercells of* $KTaO_3$ *at its experimental lattice constant*. (Note the technical details in Ref. 5 and that these LDA-derived parameters are given in Table I.) It can be clearly seen that CMC calculations yield a χ_{33} that is continuously increasing as the temperature is decreasing down to nearly 0 K. Turning on quantum effects leads to the appearance of a plateau below $\sim$100 K with a value of $\sim$100 for the dielectric constant. These CMC and PI-QMC simulations *both* predict a cubic paraelectric ground state. A plateau for the dielectric response has indeed been experimentally observed in $KTaO_3$,[2,3] but reaching a much higher dielectric constant ($\simeq$4000) and over a much narrower temperature range (i.e., below 10 K) than in Fig. 1(a).

In view of these two discrepancies, we have experimented with making minor adjustments in the LDA-fitted parameters in the hope of obtaining better agreement with experimental data. We have found that this can be done by adjusting just one of the 18 parameters, namely, the parameter denoted κ_2 in Ref. 16 which describes the harmonic part of the local-mode self-energy. (In our model, reducing κ_2 favors ferroelectricity with respect to paraelectricity since it leads to a decrease of the zone-center transverse optical frequency by weakening short-range repulsions.) Figure 1(b) shows that decreasing this single κ_2 parameter by $\sim$18% from its LDA value of 0.0866 a.u. (atomic units) leads to reasonable agreement between our PI-QMC simulations and measurements, not only for the value of the dielectric constant plateau, but also at temperatures above 10 K. (Note that the dielectric response was calculated using the correlation function approach of Refs. 17 and 18 for temperatures higher than 100 K and finite differences for T lower than 100 K. In the latter case, we used electric fields ranging between 0 and 2×10^6 V/m.)

Furthermore, this modified κ_2 also results in a dramatic difference between the two kinds of Monte-Carlo calculations. CMC simulations yield a *ferroelectric* rhombohedral

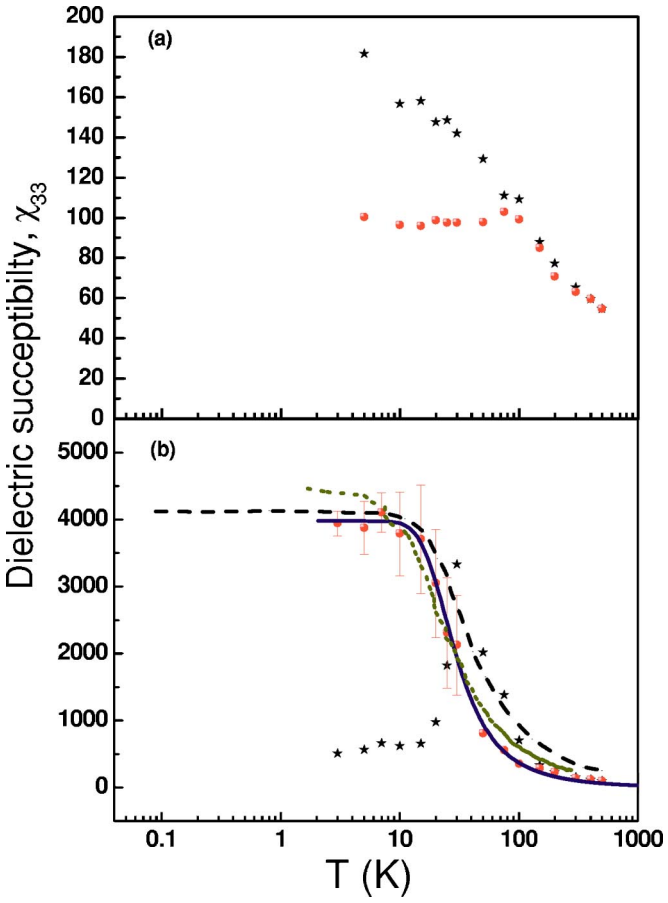

FIG. 1. (Color online) χ_{33} dielectric susceptibility of $KTaO_3$ as a function of temperature T. (a) Results for the LDA-fitted H_{eff} parameters. (b) Results for the modified set of parameters. Solid circles and stars correspond to PI-QMC and CMC results, respectively. Dashed and dotted lines represent experimental data from Refs. 2 and 3, respectively. Solid line shows the fit of the PI-QMC results by a Barrett relation, $A/[(T_1/2)\coth(T_1/2T)-T_0]$ (in Ref. 26), with $A=27\,000$, $T_1=72$ K and $T_0=29$ K. Note that our CMC simulations yield a paraelectric-to-ferroelectric transition around 30 K, which provides a numerical proof for the concept of classical Curie temperature given to T_0 in the Barrett relation.

TABLE I. The LDA-derived H_{eff} parameters in atomic units for $KTaO_3$ following the notation in Ref. 16.

	a_0	7.526[a]	Soft mode mass		95.6	
Onsite	κ_2	0.0866	α	0.26648	γ	−0.46091
Intersite	j_1	−0.02417	j_2	0.03785		
	j_3	0.00782	j_4	−0.00521	j_5	−0.00029
	j_6	0.00242	j_7	0.00121		
Elastic	B_{11}	6.51	B_{12}	0.7975	B_{44}	1.419
Coupling	B_{1xx}	−2.5179	B_{1yy}	0.4345	B_{4yz}	−0.05573
Dipole	Z^*	9.619	ε_∞	4.592[b]		

[a]Reference 6.
[b]Reference 31.

ground state. The corresponding Curie temperature is around 30 K, as evidenced by the peak in dielectric response displayed in Fig. 1(b). On the other hand, PI-QMC predicts a *paraelectric* ground state. In other words, *quantum effects suppress the paraelectric-to-ferroelectric phase transition*, which is consistent with the accepted picture.[2,3] Figures 1(a) and 1(b) thus (i) reveal that extrinsic defects (such as impurities or vacancies), which have been proposed to be responsible for the anomalous properties of $KTaO_3$,[2,3,7,8] are *not* needed to reproduce the experimental behavior of this material; and (ii) strongly suggest that, unlike in *strongly ferroelectric* perovskites,[19,20] the LDA is not accurate enough for simulating $KTaO_3$.

As for GGA, Tinte *et al.*,[6] report zone-center optical frequencies in cubic $KTaO_3$ that are all positive and close to the LDA values. According to Figs. 1(a) and 1(b), we can thus conclude that a GGA effective Hamiltonian would not provide a significant improvement over our LDA one, and will also fail in reproducing measurements. This makes $KTaO_3$ a useful test case for the development of functionals within DFT or other *ab initio* methods.

We now analyze the *microscopic* structure of $KTaO_3$ at low temperature. Figure 2 depicts the magnitude of the local modes $\mathbf{u}_i$ inside each i five-atom cell *versus* the angle that these local modes make with the pseudocubic [100] direction, as obtained from a $T=3$ K snapshot among the thermally equilibrated Monte-Carlo configurations using E_{tot} with the modified κ_2. (The magnitude of the local mode is directly proportional to the magnitude of the local polarization, e.g., $|\mathbf{u}|=0.006$ and 0.026 a.u. correspond to a local polarization $\simeq 0.0583$ and 0.253 C/m^2, respectively.) Figure 2(a) displays the CMC results, while Fig. 2(b) corresponds to PI-QMC.[27]

Comparing Figs. 2(a) and 2(b) reveals how quantum effects affect the microscopic structure of $KTaO_3$: the local polarizations go from all lying close to the [111] direction (corresponding to an angle $\simeq 54°$) and having a relatively large magnitude, to being heavily scattered in direction and having a much smaller but nonzero magnitude. The fact that $KTaO_3$ exhibits nonzero local dipoles, even when quantum fluctuations are accounted for, is consistent with the first-order lines observed in Raman spectra and which are forbidden in the ideal cubic perovskite structure.[9,10] Furthermore, an inspection of Fig. 2(b) does *not* reveal any obvious polar microregions. For instance, our quantum-statistical results do not show the local-mode distributions breaking up into clusters centered along ⟨111⟩ directions (i.e., angles of $\simeq 54°$ and/or 125°) as would be expected for such polar microregions. Incidentally, Fig. 2(b) suggests an order-disorder picture (all modes are off-site) rather than a displacive one. It also reveals that the Comes' "eight-site" model,[28] is not appropriate to describe $KTaO_3$, since the local modes lie along all possible directions.

To gain further insight into the local structure of $KTaO_3$, we decided to compute an additional set of coefficients defined as

$$\theta_\mu(\mathbf{r}) = \frac{3}{N}\sum_{i=1}^{N} \frac{u_{i,\mu}u_{i+\mathbf{r},\mu}}{|\mathbf{u_i}||\mathbf{u}_{i+\mathbf{r}}|}. \tag{1}$$

Here μ denotes the x, y, or z Cartesian axis chosen along the [100], [010], or [001] cubic directions, respectively. The index i runs over all the N B sites; $u_{i,\mu}$ and $u_{i+\mathbf{r},\mu}$ are the μ components of the local modes in cell i, and in the cell centered at a distance $\mathbf{r}$ from cell i, respectively. The case in which the local dipoles all have the same (nonzero) magni-

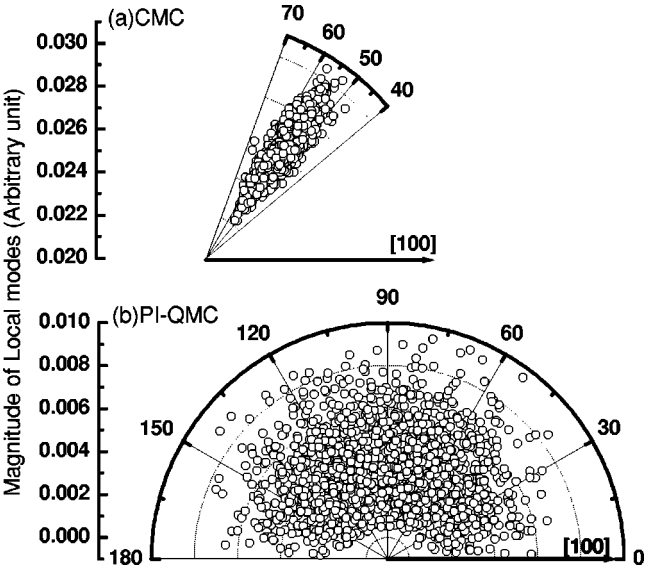

FIG. 2. Magnitude of local modes of $KTaO_3$ at T=3 K vs the angle that these modes make with respect to the [100] pseudocubic direction. The modified set of H_{eff} parameters is used.

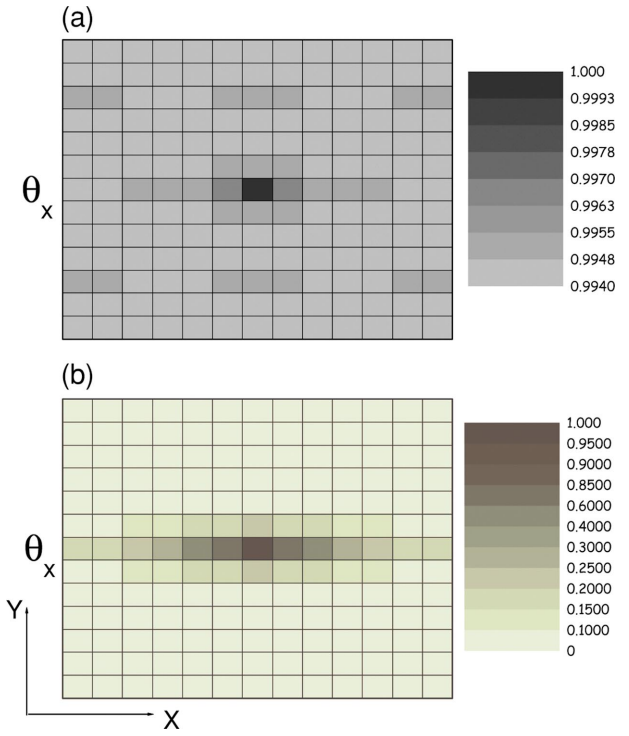

FIG. 3. (Color) Correlation function $\theta_x(\mathbf{r})$ of Eq. (1) for $KTaO_3$ plotted in the *x*-*y* plane for a $12\times12\times12$ simulation at $T=3$ K. (a) CMC results; (b) PI-QMC results. Each small square represents one lattice B site; the origin lies at the center. The modified set of H_{eff} parameters is used. Note that the color scales are different in the two panels.

tude and are all aligned along a given $\langle 111\rangle$ direction yields a value of 1 for $\theta_\mu(\mathbf{r})$, for any $\mathbf{r}$ and for any μ. This case corresponds to a ferroelectric rhombohedral state having identical local and average structures. On the other hand, the other limiting case—for which neighbors at a distance $\mathbf{r}$ do not exhibit any correlation between the μ components of their local modes—is associated with a zero value for $\theta_\mu(\mathbf{r})$.

Figure 3 depicts $\theta_x(\mathbf{r})$ (i.e., $\mu=x$) for $\mathbf{r}$ lying in the *x*-*y* plane. The results correspond to one snapshot of a thermally equilibrated Monte Carlo configuration at $T=3$ K, using the H_{eff} approach with the modified κ_2. Panels (a) and (b) correspond to CMC and PI-QMC simulations, respectively.

The CMC technique leads to a $\theta_x(\mathbf{r})$ close to unity for any $\mathbf{r}$, and thus generates a macroscopically and microscopically ferroelectric rhombohedral structure, as consistent with Fig. 2(a). On the other hand, PI-QMC simulations give a more complex behavior for $\theta_x(\mathbf{r})$ at low temperature. One can see that the *x* components of the local modes are *longitudinally* correlated in a *needle-like* fashion: $\theta_x(\mathbf{r})$ adopts large values only when $\mathbf{r}$ is along the [100] direction. These values decrease as the magnitude of $\mathbf{r}$ increases. [The same result is obtained for all symmetry related cases, e.g., for $\theta_x(\mathbf{r})$ in the *x*-*z* plane, etc.] Figure 2(b) further reveals that $\theta_x(\mathbf{r})\simeq0.5$ for neighbors at a distance of $\pm2a$ (where $a\simeq4$ Å is the cubic lattice constant) along the *x* axis. This is in good agreement with the characteristic size of 16 Å extracted from low-temperature Raman spectra of $KTaO_3$.[9] On the other hand, our simulations go against the hypothesis of isotropic correlation made in Ref. 9. The longitudinal needle-like correlations depicted in Fig. 3(b) have also been predicted to occur in classical ferroelectrics just above the paraelectric-to-ferroelectric transition temperature.[29] In fact, they are pretransitional effects that are probably common to most ferroelectric perovskites, the peculiarities of quantum paraelectric $KTaO_3$ being that the phase transition does not actually occur and that the needle-like correlations result in a plateau for the dielectric response. Finally, note that these needle-like correlations are consistent with the peculiar diffuse x-ray scattering observed in Ref. 12.

IV. CONCLUSIONS

We have performed large-scale atomistic simulations to investigate the (defect-free) incipient ferroelectric $KTaO_3$ system using a parameterized effective-Hamiltonian approach. The effect of quantum-mechanical zero-point motion is investigated by comparing the results of classical and path-integral Monte Carlo simulations. We find that the fitting of all the H_{eff} parameters within LDA yields a theoretical dielectric constant that is in poor quantitative agreement with experiment, strongly suggesting that LDA is inadequate for this material. Results in the literature also indicate that GGA will not improve the LDA result. On the other hand, a small modification of a single parameter in H_{eff} from its LDA value is enough to obtain reasonable agreement between theory and experiment for the dielectric constant over a wide temperature range. This modified H_{eff} leads to the predictions that (i) $KTaO_3$ is ferroelectric classically, but becomes paraelectric once zero-point phonon vibrations are included, and (ii) the quantum-induced local structure of $KTaO_3$ is characterized by nonzero local dipoles that have longitudinal, needle-like correlations with a correlation length spanning a few unit cells. Finally, our work provides a basis for a theoretical framework to tackle compositionally disordered alloys, based on incipient ferroelectrics,[30] which *do* exhibit ferroelectric phases.

ACKNOWLEDGMENTS

The authors thank D. Ceperley, B. Dkhil, M. Itoh, J. M. Kiat, W. Kleemann, J. Kohanoff, I. Kornev, S. A. Prosandeev, G. Samara, J. Shumway, and E. Venturini for useful discussions. This work was supported by Office of Naval Research Grant Nos. N00014-01-1-0365 (CPD), N00014-01-1-0600, and N00014-97-1-0048, National Science Foundation Grant No. DMR-9983678, and Department of Energy Contract No. DE-AC04-94AL85000 at Sandia National Laboratories.

[1] O. E. Kvyatkovskiĭ, Phys. Solid State **43**, 1401 (2001).
[2] B. Salce, J. L. Gravil, and L. A. Boatner, J. Phys.: Condens. Matter **6**, 4077 (1994).
[3] S. H. Wemple, Phys. Rev. **137**, A1575 (1964).
[4] D. J. Singh, Phys. Rev. B **53**, 176 (1996).
[5] K. Leung, Phys. Rev. B **63**, 134415 (2001).
[6] S. Tinte, M. G. Stachiotti, C. O. Rodiguez, D. L. Novikov, and N. E. Christensen, Phys. Rev. B **58**, 11 959 (1998).
[7] S. Rod, F. Borsa, and J. J. Van der Klink, Phys. Rev. B **38**, 2267 (1988).
[8] P. Grenier, G. Bernier, S. Jandl, B. Salce, and L. A. Boatner, J. Phys.: Condens. Matter **1**, 2515 (1989).
[9] H. Uwe, K. B. Lyons, H. L. Carter, and P. A. Fleury, Phys. Rev. B **33**, 6436 (1986).
[10] J. Toulouse, P. DiAntonio, B. E. Vugmeisterm, X. M. Wang, and L. A. Knauss, Phys. Rev. Lett. **68**, 232 (1992).
[11] C. Ang, A. S. Bhalla, and L. E. Cross, Phys. Rev. B **64**, 184104 (2001).
[12] R. Comès and G. Shirane, Phys. Rev. B **5**, 1886 (1972).
[13] P. Hohenberg and W. Kohn, Phys. Rev. **136**, B864 (1964); W. Kohn and L. J. Sham, Phys. Rev. **140**, A1133 (1965).
[14] J. P. Perdew and Y. Wang, Phys. Rev. B **45**, 13 244 (1992).
[15] J. P. Perdew, K. Burke, and M. Ernzerhof, Phys. Rev. Lett. **77**, 3865 (1996).
[16] W. Zhong, D. Vanderbilt, and K. M. Rabe, Phys. Rev. Lett. **73**, 1861 (1994); Phys. Rev. B **52**, 6301 (1995).
[17] A. García and D. Vanderbilt, in *First-Principles Calculations for Ferroelectrics: Fifth Williamsburg Workshop*, edited by R. E. Cohen (AIP, Woodbury, NY, 1998), p. 53.
[18] A. García and D. Vanderbilt, Appl. Phys. Lett. **72**, 2981 (1998).
[19] D. Vanderbilt, Curr. Opin. Solid State Mater. Sci. **2**, 701 (1997).
[20] L. Bellaiche, Curr. Opin. Solid State Mater. Sci. **6**, 19 (2002).
[21] J. Íñiguez and D. Vanderbilt, Phys. Rev. Lett. **89**, 115503 (2002).
[22] K. Leung, E. Cockayne, and A. F. Wright, Phys. Rev. B **65**, 214111 (2002).
[23] N. Metropolis, A. W. Rosenbluth, M. N. Rosenbluth, A. H. Teller, and E. Teller, J. Chem. Phys. **21**, 1087 (1953).
[24] W. Zhong and D. Vanderbilt, Phys. Rev. B **53**, 5047 (1996).
[25] D. M. Ceperley, Rev. Mod. Phys. **67**, 279 (1995).
[26] J. H. Barrett, Phys. Rev. **86**, 118 (1952).
[27] Starting from the path-integral form of the partition function, it can be shown that the local modes $\mathbf{u}_i(t)$ are to be averaged over imaginary time before computing static quantities such as the local mode distributions of Fig. 2(b) or the correlations defined by Eq. (1). Hence, it is not correct to compute these quantities at different imaginary times and then average over t.
[28] R. Comes, M. Lambert, and A. Guinier, C. R. Acad. Sci. Paris **266**, 959 (1968); Solid State Commun. **6**, 715 (1968); J. P. Sokoloff, L. L. Chase, and D. Rytz, Phys. Rev. B **38**, 597 (1988).
[29] D. Vanderbilt, and W. Zhong, Ferroelectrics **206-207**, 181 (1998).
[30] G. A. Samara, J. Phys.: Condens. Matter **15**, R367 (2003).
[31] M. Exner, H. Donnerberg, C. R. A. Catlow, and O. F. Schirmer, Phys. Rev. B **52**, 3930 (1995).